Determining concentration depth profiles in fluorinated networks by means of electric force microscopy

Luis A. Miccio,[1,2,a)] Mohammed M. Kummali,[2,3] Pablo E. Montemartini,[1] Patricia A. Oyanguren,[1] Gustavo A. Schwartz,[2] Ángel Alegría,[2,3] and Juan Colmenero[2,3,4]
[1]*Institute of Materials Science and Technology (INTEMA), University of Mar del Plata and National Research Council (CONICET), JB. Justo 4302, Mar del Plata, Buenos Aires, Argentina*
[2]*Centro de Física de Materiales CSIC-UPV/EHU, Materials Physics Center (MPC), Paseo Manuel de Lardizabal 5, 20018 San Sebastian, Spain*
[3]*Departamento de Física de Materiales UPV/EHU, Facultad de Química, 20080 San Sebastián, Spain*
[4]*Donostia International Physics Center, Paseo Manuel de Lardizabal 4, 20018 San Sebastián, Spain*

(Received 2 May 2011; accepted 20 July 2011; published online 11 August 2011)

By means of electric force microscopy, composition depth profiles were measured with nanometric resolution for a series of fluorinated networks. By mapping the dielectric permittivity along a line going from the surface to the bulk, we were able to experimentally access to the fluorine concentration profile. Obtained data show composition gradient lengths ranging from 30 nm to 80 nm in the near surface area for samples containing from 0.5 to 5 wt. % F, respectively. In contrast, no gradients of concentration were detected in bulk. This method has several advantages over other techniques because it allows profiling directly on a sectional cut of the sample. By combining the obtained results with x-ray photoelectron spectroscopy measurements, we were also able to quantify F/C ratio as a function of depth with nanoscale resolution. © *2011 American Institute of Physics*. [doi:10.1063/1.3624574]

I. INTRODUCTION

Fluorinated polymers are extensively applied as high-performance coatings to obtain water-/oil-repellent, antifouling, low-friction, and non-sticky surfaces.[1,2] Due to the unique properties achieved, surface segregation of fluorinated species has been used to obtain polymeric coatings with low surface energy and interesting bulk properties.[3,4] Knowledge of depth composition profile for this kind of materials is critical from a scientific as wells as technological point of view, and thus, nanoscale depth profiling techniques are essential in the characterization process. Moreover, composition profiles are valued in scaling theories or self-consistent field calculations, for comparison and material characterization purposes.[5]

Over the last few years, several techniques have been extensively used for determining composition profiles in polymers, including: angle-resolved x-ray photoelectron spectroscopy (ARXPS), nuclear magnetic resonance (NMR), energy-dispersive x-ray spectroscopy (EDXS), neutron reflectometry (NR), and dynamic secondary ion mass spectrometry (DSIMS). During the past two decades, ARXPS has been developed and applied to many practical problems;[6] it can provide information up to 10 nm below the surface. On the other hand, EDXS can be coupled with SEM for detecting species with atomic numbers greater than 4; however, its minimum penetration depth in polymers is in the range of thousands of nm.[7] NMR can be used for concentration depth profiling of hydrogen and fluorine in polymer films at room temperature, with a spatial resolution of approximately 5 μm.[8] The DSIMS technique can also be used on polymeric samples to extract valuable information from the near-surface region, but only by applying a sacrificial layer on top of the studied polymer.[9,10] NR is another interesting technique for profiling polymers, but in this case, the required contrast between the matrix and the molecule of interest can be achieved only by deuterating the latter.[5] Furthermore, since all these techniques lack nanometric spatial resolution, concentration profiles in sectional cuts of samples cannot be obtained. On the other hand, the depth profiles obtained during perpendicular measurements can be strongly influenced by the irregular topography of the sample.

AFM based techniques are in principle attractive looking for nanoscale resolution. Particularly, a new technique based on electric force microscopy (EFM) has been recently developed;[11–14] this technique can provide quantitative information about the local dielectric permittivity of the sample by combining the so-called double-pass method with a numerical model.[15–19] EFM is sensitive to dielectric permittivity contrast and, therefore, can be used to determine concentration profiles given a significant variation due to compositional differences. Thus, in this work, we report a method for obtaining concentration depth profiles in fluorinated polymer networks by means of EFM. We take advantage of the high spatial resolution of the atomic force microscopy and the high sensitivity of EFM to detect fluorine moieties, through the low polarizability of the C–F bond. As a result, by mapping the local variations of the dielectric permittivity along a line going from the surface to the bulk, we are able to experimentally access the fluorine concentration profile with nanoscale resolution.

[a)]Author to whom correspondence should be addressed. Electronic mail: luisalejandro_miccio@ehu.es. Telephone: +34943018779.

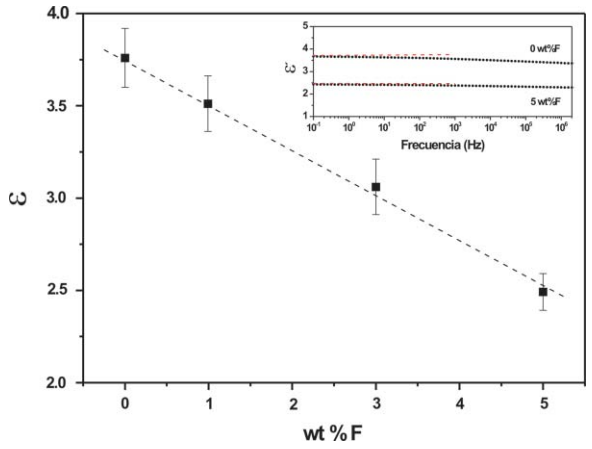

FIG. 1. Dielectric permittivity as a function of wt. % F measured at room temperature for samples containing 0, 1, 3, and 5 wt. % F. The line is just a guide for the eyes. The inset shows the area used to determine the dielectric permittivity of the materials.

II. EXPERIMENTAL DETAILS

A. Sample preparation

Polymer networks with different fluorine concentration were synthesized by two steps, (1) reaction of a perfluorinated epoxy with a known excess of a tetrafunctional amine and (2) curing the product with a difunctional epoxy. Differences in fluorine concentration between surface and bulk for this kind of polymers have been previously studied.[20,21] Samples were prepared by varying the weight percentage of F from zero to five namely: 0.5, 1, 3, and 5 wt. % F.

B. Macroscopic permittivity

In order to confirm a significant dielectric contrast between the polymeric matrix and the fluorinated species, the macroscopic permittivity of fluorinated samples was measured by standard broadband dielectric spectroscopy (BDS). Disk shaped samples (containing 0 to 5 wt. % F) with 20 mm diameter and 0.5 mm thickness were measured at several temperatures in the range 10^{-1}–10^{7} Hz (Novocontrol Alpha A impedance analyzer). The dielectric permittivity was then determined at room temperature at the low frequency limit, where the response was found to be nearly frequency independent.

As shown in Fig. 1, the dielectric permittivity decreases almost linearly with increasing fluorine concentration, in agreement with previous studies.[22] These results indicate that we should detect a clear dielectric contrast between the bulk and the surface, where the difference of fluorine concentration is even larger.

C. EFM experimental setup

Polymer sheets having a thickness of about 200 μm were obtained with a microtome (Leica RM2255). In order to minimize the mechanical perturbations, the cutting direction was rigorously perpendicular to the surface of the sample (Fig. 2(a)). Finally, to ensure good electrical contact between the polymeric material and the sample-holder, the bottom surface of the sample was gold sputtered (Fig. 2(b)).

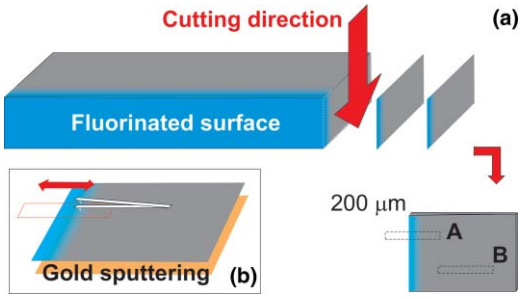

FIG. 2. Scheme of the sample preparation procedure. (a) Sheets of 200 μm were cut with a microtome in perpendicular direction to the fluorine gradient (fluorine rich surface in blue and bulk in grey). A and B are the analyzed areas of each sample. (b) The sample was scanned with an aspect ratio of 1:10 (the bottom surface was gold sputtered).

The topographic profile and the electrical interaction profile were recorded simultaneously with an atomic force microscope multimode V (Veeco) operating in EFM mode. Near surface (region A) and bulk (region B) areas (Fig. 2(a)) on each sample were scanned several times. For each line of the image, we perform two scans (double pass method); during the first scan, tapping mode provides the topography of the sample, whereas during the second scan the tip follows the recorded topography, at a lift height of 10 nm, (lift mode). At this point, a bias voltage is applied to the tip and the resonance frequency shift induced by the electrical force gradient is then measured.[17]

In order to emphasize the concentration depth profiles, we have chosen an aspect ratio of 1:10 for the scanned area. The cantilevers (SCM–PIT tips from Bruker) used during the measurements were made of antimony (n) doped Si, coated with Pt/Ir. The natural frequencies were in the range of 70–80 kHz and their stiffness were found to be in the range 1.5–3 N/m.

III. DATA TREATMENT

The voltage applied to the tip during the lift mode in the double pass method (V_{dc}) causes a force gradient according to

$$\nabla F = \frac{1}{2}\frac{\partial^2 C(z,\varepsilon)}{\partial z^2}(V_{dc})^2. \quad (1)$$

As a result, this force gradient produces in turn a shift in the resonance frequency of the cantilever (Δf) according to

$$\Delta f = -\tfrac{1}{2}\cdot f_0 \cdot \nabla F \cdot k_c^{-1}, \quad (2)$$

where k_c and f_o are the stiffness and the natural resonance frequency of the cantilever, respectively. Therefore, Δf can be related to the dielectric permittivity of the sample through the tip-sample capacitance (C).[17] Moreover, the detected frequency shift depends on the square of the applied voltage. Thus, for a small tip-sample distance and fixed V_{dc}, the dielectric permittivity of the sample is nearly proportional to the detected frequency shift.[23] Therefore, we assumed that $\partial^2 C(z,\varepsilon)/\partial^2 z$ is approximately proportional to an effective permittivity ε_{eff}. In this approximation, for EFM

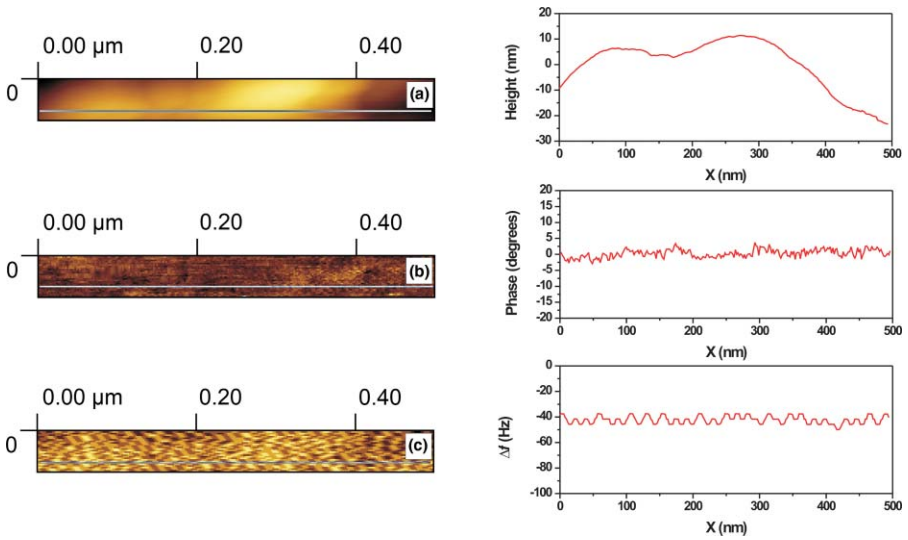

FIG. 3. (a) Height image and profile of interior area (region B in Fig. 2(a)) for a sample containing 1 wt. % F. (b) Corresponding phase image and profile. (c) Corresponding frequency shift image and profile.

experiments on bulk we assign $\varepsilon_{eff} \cong \varepsilon_{Bulk}$, where ε_{Bulk} is the macroscopic dielectric permittivity. In this way, in the near surface area we can relate the variation of ε_{eff} with the variation of Δf as $\varepsilon_{eff} = \Delta f / \Delta f_{Bulk}\, \varepsilon_{Bulk}$.

IV. RESULTS AND DISCUSSION

Rather flat Δf profiles were observed when scanning on bulk areas (region B in Fig. 2(a)). Figure 3 shows height, phase, and frequency shift images for a sample containing 1 wt. % F scanned in area B with a tip bias of 2 V. Figure 3(c), shows a constant shift in frequency implying that the electrical interaction between the tip and the sample remains constant throughout the whole region. On the other hand, Fig. 4 shows height, phase, and frequency shift images of the near surface area (region A in Fig. 2(a)) of a sample containing 5 wt. % F for a tip bias of 2 V. The Δf increases continuously (higher negative values) with increasing depth up to a few tens of nm away from the surface, indicating the beginning of the bulk.

Figure 5 shows the obtained profiles for samples containing 1 wt. % F (Fig. 5(a)) and 5 wt. % F (Fig. 5(b)) for tip bias 0, 0.5, 1, and 2 V (from top down). On the right, the frequency shift is plotted as a function of bias voltage for surface (black) and bulk (red) areas of both samples. As the bias voltage increases the detected Δf, signal increases parabolically as predicted by Eq. (1). Measurements were performed for higher values of tip bias as well. However, the best signal/noise ratio for the analyzed materials was found to be at 2 V. This might be because higher voltages affect the tip-sample distance during the lift mode. Furthermore, for neat samples (0 wt. % F), no such gradients were detected either in A or B areas, all confirming that the detected changes of Δf must be attributed to local variations in the fluorine content.

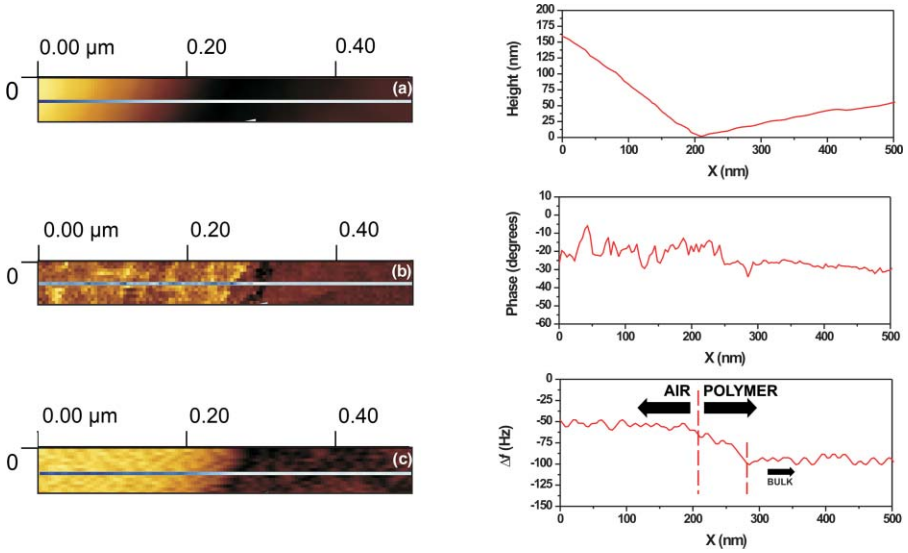

FIG. 4. (a) Height image and profile of near surface area (region A in Fig. 2(a)) for a sample containing 5 wt. % F. (b) Corresponding phase image and profile. (c) Corresponding frequency shift image and profile (tip bias 2 V).

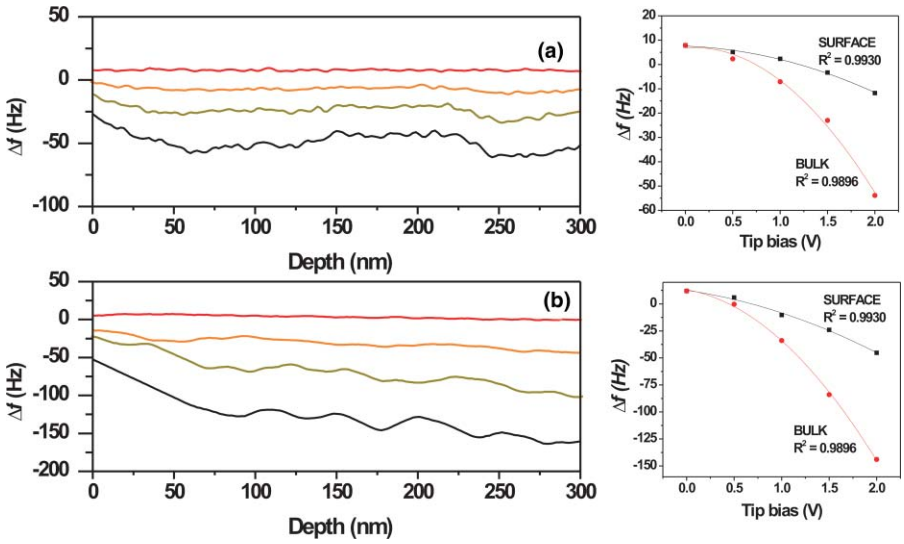

FIG. 5. Frequency shift profiles obtained at 0, 1, 1.5, and 2 V (seen from top down). (a) Sample containing 1 wt. % F. (b) Sample containing 5 wt. % F. On the right, the frequency shift is plotted as a function of bias voltage for surface (black) and bulk (red) areas of both samples.

According to Fig. 1, higher dielectric permittivity means lower fluorine content. Hence, the fluorine-rich surface has lower Δf values compared to bulk values (as is clear from Fig. 5). Moreover, the constant Δf value observed for bulk (in A region) shows that the fluorine concentration is also constantly a few tens of nanometers below the surface.

In order to quantify the F/C ratio, the Δf variations were scaled using XPS data previously obtained for the same samples.[21] Figure 6(a) shows the corresponding values of the ε_{eff} for the samples here analyzed. At this point, we scaled ε_{eff} to the F/C ratio measured by XPS for each sample by fitting with an exponential decay function ($y = a \cdot e^{b \cdot x}$),[21] as shown in Fig. 6(b). Finally, the F/C concentration profile as a function of depth can be obtained by combining Figs. 6(a) and 6(b), as shown in Fig. 6(c).

The gradient length decreases when fluorine content decreases. F/C gradients of about 25, 30, 60, and 80 nm were observed for samples with 0.5, 1, 3, and 5 wt. % F, respectively. These results can be rationalized by considering two opposite thermodynamic effects. On the one hand, there is an entropic penalty which arises from the restriction of chain configurations in the gradient. On the other hand, there is a lowering of free energy by enriching the surface with fluorine. A balance of both these define the shape of the concentration profile. Therefore, as concentrated samples have higher surface enrichment, the profile depths are also higher in order to reach bulk composition minimizing entropy penalties, resulting in a rather similar slope of the concentration profile.

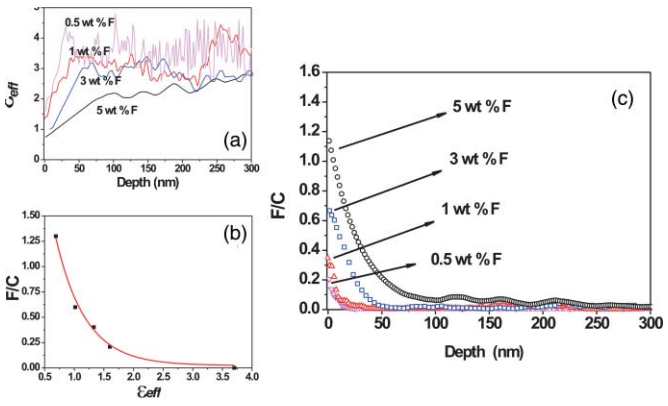

FIG. 6. (a) Normalized profiles (ε_{eff} vs depth) for samples containing 0.5, 1, 3, and 5 wt. % F at a constant tip bias (2 V). These results were obtained by assuming $\varepsilon_{eff} = \Delta f / \Delta f_{Bulk}\, \varepsilon_{Bulk}$, where ε_{Bulk} is the macroscopic dielectric permittivity and Δf_{Bulk} is the frequency shift at bulk area (A) in Fig. 2(a). (b) Scaling curve ε_{eff} to F/C ratio (obtained through XPS). (c) F/C vs depth profiles, obtained after combining normalized and scaling curves.

V. CONCLUSIONS

Concentration depth profiles for different fluorinated samples were mapped using EFM. This procedure allows detecting profiles directly on a sectional cut due to the high spatial resolution of the AFM and it can be applied successfully to any material having dielectric contrast between the constituent species. This procedure is less sensitive to perturbations produced by sample preparation because it measures the electrical interactions in a volumetric spot of sample. Consequently, it has great advantages over mechanical AFM measurements that preferentially probe the first layers on the surface of the specimen. This method clearly paves the way for a complete polymer modeling and characterization and opens an interesting new use for electric force microscopy.

ACKNOWLEDGMENTS

L.A.M., M.M.K., G.A.S., A.A., and J.C. acknowledge the financial support provided by the Basque Country Government (Grant No. IT-436-07), the Spanish Ministry of Science and Innovation (Grant Nos. MAT 2007-63681 and CSD 2006-00053). The Donostia International Physics Center (DIPC) financial support is also acknowledged.

[1]A. G. Pittman, *Fluoropolymers* (Wiley, New York, 1972).
[2]M. N. Coelho, E. P. Vieira, H. Motschmann, H. Mohwald, and A. F. Thunemann, Langmuir **19**, 7544 (2003).
[3]T. Dikic, S. J. F. Erich, W. Ming, H. P. Huinink, P. C. Thüne, R. A. T. M. van Benthem, and G. de With, Polymer **48**, 4063 (2007).
[4]Ph. Game, D. Sage, and J. P. Chapel, Macromolecules **35**, 917 (2002).
[5]I. Hopkinson, F. T. Kiff, R. W. Richards, D. G. Bucknall, and A. S. Clough, Polymer **38**, 87 (1997).
[6]C. J. Powell and A. Jablonski, J. Electron Spectrosc. Relat. Phenom. **178–179**, 331 (2010).
[7]J. Goldstein, D. E. Newbury, D. C. Joy, C. E. Lyman, P. Echlin, E. Lifshin, L. Sawyer, and J. R. Michael, *Scanning Electron Microscopy and X-Ray Microanalysis*, 3rd ed. (Springer, New York, 2003), p. 586.
[8]S. J. F. Erich, J. Laven, L. Pel, H. P. Huinink, and K. Kopinga, Prog. Org. Coat. **55**(2), 105 (2006).
[9]H. Yokoyama, E. J. Kramer, M. H. Rafailovich, J. Sokolov, and S. A. Schwarz, Macromolecules **31**, 8826 (1998).
[10]X. Hu, W. Zhang, M. Si, M. Gelfer, B. Hsiao, M. Rafailovich, J. Sokolov, V. Zaitsev, and S. Schwarz, Macromolecules **36**, 823 (2003).
[11]P. S. Crider, M. R. Majewski, J. Zhang, H. Oukris, and N. E. Israeloff, Appl. Phys. Lett. **91**, 013102 (2007).
[12]P. S. Crider, M. R. Majewski, J. Zhang, H. Oukris, and N. E. Israeloff, J. Chem. Phys. **128**, 044908 (2008).
[13]A. V. Krayev and R. V. Talroze, Polymer **45**, 8195 (2004).
[14]A. V. Krayev, G. A. Shandryuk, L. N. Grigorov, and R. V. Talroze, Macromol. Chem. Phys. **207**, 966 (2006).
[15]C. Riedel, R. Arinero, Ph. Tordjeman, M. Ramonda, G. Lévêque, G. A. Schwartz, D. G. De Oteyza, A. Alegria, and J. Colmenero, J. Appl. Phys. **106**, 024315 (2009).
[16]C. Riedel, R. Arinero, Ph. Tordjeman, G. Lévêque, G. A. Schwartz, A. Alegría, and J. Colmenero, Phys. Rev. E **81**, 010801 (2010).
[17]C. Riedel, G. A. Schwartz, R. Arinero, Ph. Tordjeman, G. Lévêque, A. Alegría, and J. Colmenero, Ultramicroscopy **110**, 634 (2010).
[18]C. Riedel, R. Sweeney, N. E. Israeloff, R. Arinero, G. A. Schwartz, A. Alegría, Ph. Tordjeman, and J. Colmenero, Appl. Phys. Lett. **96**, 213110 (2010).
[19]M. M. Kummali, G. A. Schwartz, A. Angel, R. Arinero, J. Colmenero, "Compatibility studies of poly(styrene) and poly(vinyl acetate) blends using electrostatic force microscopy," J. Polym. Sci., Part B: Polym. Phys. (to be published).
[20]L. A. Miccio, D. Fasce, W. Schreiner, P. E. Montemartini, and P. A. Oyanguren, Eur. Polym. J. **46**, 744 (2010).
[21]L. A. Miccio, R. Liaño, W. Schreiner, P. E. Montemartini, and P. A. Oyanguren, Polymer **51**, 6219 (2010).
[22]H. Jung and H. Park, Thin Solid Films **420–421**, 248 (2002).
[23]G. Gomila, J. Toset, and L. Fumagalli, J. Appl. Phys. **104**, 024315 (2008).